Radiol Phys Technol (2016) 9:202–213
DOI 10.1007/s12194-016-0349-2

Effect of fluence smoothing on the quality of intensity-modulated radiation treatment plans

Puzhakkal Niyas[1,2,3] · Kallikuzhiyil Kochunny Abdullah[1] · Manthala Padannayil Noufal[1,2,3] · Thekkedath Sankaran Nair[2]

Received: 26 October 2015 / Revised: 18 February 2016 / Accepted: 19 February 2016 / Published online: 7 March 2016

Abstract A fluence-smoothing function applied for reducing the complexity of a treatment plan is an optional requirement in the inverse planning optimization algorithm of intensity-modulated radiation therapy (IMRT). In this study, we investigated the consequences of fluence smoothing on the quality of highly complex and inhomogeneous plans in a treatment-planning system, Eclipse^{TM}. The smoothing function was applied both in the direction of leaf travel (X) and perpendicular to leaf travel (Y). Twenty IMRT plans from patients with cancer of the nasopharynx and lung were selected and re-optimized with use of various smoothing combinations from $X = 0$, $Y = 0$ to $X = 100$, $Y = 100$. Total monitor units (MUs), dose–volume histograms, and radiobiological estimates were computed for all plans. The study yielded a significant reduction in the average total MUs from 2079 ± 265.4 to 1107 ± 137.4 (nasopharynx) and from 1556 ± 490.3 to 791 ± 176.8 (lung) while increasing smoothing from X, $Y = 0$ to X, $Y = 100$. Both the tumor control and normal tissue complication probabilities were found to vary, but not significantly so. No appreciable differences in doses to the target and most of the organs at risk (OARs) were noticed. The doses measured with the I'MRT MatriXX 2-D system indicated improvements in deliverability of the plans with higher smoothing values. Hence, it can be concluded that increased smoothing reduced the total MUs exceptionally well without any considerable changes in OAR doses. The observed progress in plan deliverability in terms of the gamma index strongly supports the recommendation of smoothing levels up to $X = 70$ and $Y = 60$, at least for the nasopharynx and lung.

Keywords IMRT · Monitor units (MUs) · Fluence smoothing · DVH · EUD

1 Introduction

Radiation therapy uses ionizing radiation to inhibit the functioning and multiplication of tumor cells. External-beam radiation therapy has been found to be beneficial for 52 % of all cancer patients [1]. The objective of radiation therapy is to deliver a prescribed amount of lethal radiation dose to the tumor while minimizing the dose to surrounding normal tissues. This has been achieved with the help of a technique called intensity-modulated radiation therapy (IMRT), which generally uses inverse planning with an optimization algorithm to reach the desired dose distribution to the planning target volume (PTV) and a low dose to the surrounding organs at risk (OARs). After fixing the number of beams, and their directions and defining constraints on the doses to the PTVs and the OARs, the computerized treatment planning system (TPS) creates a large numbers of beamlets. The fluences of these beamlets are optimized by use of inverse-planning algorithms. There are two different approaches for optimization of IMRT planning. In the traditional two-step optimization process, the beamlet fluences are first optimized to produce an "optimal fluence map" by use of iterative reconstruction. The leaf motion calculator (LMC) creates the multi-leaf collimator (MLC) positions and accounts for physical and

✉ Puzhakkal Niyas
pniyas@gmail.com

[1] Department of Physics, Farook College, Kozhikode, Kerala 673632, India

[2] Department of Medical Physics and Radiation Oncology, Baby Memorial Hospital, Kozhikode, Kerala 673004, India

[3] University of Calicut, Malappuram, Kerala 673635, India

mechanical constraints on the MLC such as leaf transmission, maximum leaf speed, and leaf edge shape. Because of these limitations, more complex plans are more difficult to achieve, and the LMC creates an "actual fluence map" which is as close to the "optimal fluence map" as possible [2]. In the second approach, direct machine parameter optimization (DMPO), the MLC constraints are taken into account in the optimization process itself, and deliverable treatment plans are optimized in a single step [3, 4]. As there is no conversion of the fluence map at the end of the optimization, the planner has better control over the complexity of plans than is possible with two-step optimization. The term "complexity" can be described as the degree of frequency fluctuations and the amplitude in the fluence distribution of the beam [5]. Depending on the geometry of the PTVs and the OARs, the demands for conformity to the PTV, and the tolerance of the surrounding OARs, the fluence maps can be correspondingly complex. If the complexity is reduced, this implies that the quality of the treatment plan may deteriorate because of loss in the conformity or because of unacceptable doses to OARs. However, more complex plans cause greater practical difficulties for the delivery system. Increased complexity of the delivered fluence map will result in a large number of monitor units (MUs). This addresses challenges such as long-term secondary cancer induction [6], increased skin dose, a longer treatment time, and uncertainties during treatment delivery. These potential consequences can be minimized by use of several methods which reduce the complexity of treatment plans. Such methods are known as "smoothing" of the delivered intensity maps [7–11].

Two recommended methods of fluence map smoothing are (1) the use of intensity-modulated beam (IMB) smoothing filters and (2) inclusion of smoothness terms into the objective function of the optimization algorithm. Both these methods reduce fluence variations between adjacent beamlets by eliminating noise in the fluence maps. Commercially available treatment-planning systems typically include a smoothing interface by which the user can adjust the smoothing parameters for different levels of fluence smoothing. Most TPS vendors recommend the use of a default set of smoothing parameters within their software, which leads to a moderate level of smoothing. However, it has been observed that a change in default smoothing levels results in a change in both plan quality and treatment efficiency in terms of the integral dose [12]. These effects will vary with treatment sites.

In the current study, we evaluated the effect of such smoothing functions in Varian Eclipse™ TPS, version 10.0 (Varian Medical Systems, Palo Alto, CA, USA) for 20 IMRT cases at two complex sites treated in our radiation therapy center. We also investigated the improvements in the plan quality for these two sites while varying the fluence smoothness, and we recommend an optimum smoothing parameter for the particular anatomic regions.

2 Materials and methods

For understanding the effect of the smoothing parameters in the inverse TPS, it is very important to know how a TPS performs fluence smoothing within its inverse-planning process. In Eclipse™, fluence smoothing is attained within the objective function of the TPS [13]. A user can define dose–volume constraints, their priorities, and the smoothing values in both the direction of leaf travel (X) and the direction perpendicular to leaf travel (Y). Smoothing is applied at each iteration by addition of a smoothing weighted objective in the cost function, and the total objective function becomes a combination of two terms [14]:

$$F(x) = \sum_i w_i (D_i - P_i)^2 + \sum_k w_k (x_{k+1} - x_k)^2 \cdot \quad (1)$$

The first term is the usual component for dose–volume constraints. P_i is the prescribed dose of the ith voxel, w_i is the weight (priority) factor given to particular objective, and D_i is the computed dose at point i. D_i is expressed as follows:

$$D_i = \sum_i d_{j,i} \cdot x_j, \quad (2)$$

where $d_{j,i}$ is the dose to point i from the jth beamlet, and x_j is the jth beamlet weight in the fluence map. The second term in Eq. (1) is related to the smoothing, and is used to reduce excessive fluence differences between adjacent bixels in the X or Y direction. The two weights w_k (X and Y smoothing values) determine the relative priority of these goals in the total objective function. For each beamlet, the fluence value differences between adjacent pencil beams are summed together and then multiplied by user-defined X and Y smoothing values, which are then added to the penalty score of the total objective function. Thus, the fluence-smoothing process increases the total value of the objective function penalty score for plans with broadly varying fluence maps, thereby guiding the optimization, toward smoother fluence maps [12].

Our total of 20 cases consisted of 10 patients with carcinoma of the nasopharynx and 10 patients with carcinoma of the lung. These patients had already completed their treatments in our radiation therapy center with use of a Varian clinac-iX LINAC with a 120 leaf millennium MLC (Varian Medical Systems, Palo Alto, CA, USA). Treatments were delivered by inverse planned dynamic-IMRT techniques. All of the investigated nasopharynx cases were treated with a dose of 212.1 cGy/fraction (total

dose = 7000 cGy). The lung patients were treated with 200 cGy/fraction (total dose = 6000 cGy). All of these treatment plans had nine and seven static beam angles for the nasopharynx and lung, respectively. Figure 1 shows examples of dose distributions for the nasopharynx and lung plans. The plans were produced in the Varian Eclipse^{TM} TPS with 6-MV-energy beams in two-step optimization by use of vendor-default smoothing values. Each of these approved and verified plans was used as a reference plan for evaluation of newly created treatment plans. The reference plans were then copied and modified by use of different X and Y smoothing parameters which varied from 0 to 100. A total of nine plans with smoothing at ($X = 0$, $Y = 0$; vendor-defined minimum), ($X = 20$, $Y = 10$), ($X = 40$, $Y = 30$; vendor-default), ($X = 50$, $Y = 40$), ($X = 60$, $Y = 50$), ($X = 70$, $Y = 60$), ($X = 80$, $Y = 70$), ($X = 90$, $Y = 80$) and ($X = 100$, $Y = 100$; maximum defined in standard practice [15]) were created for all patients. Even though the range of possible smoothing levels in Eclipse is 0–999, in this study we duplicated the range and interval used by a previous author, Armoogum [16], for better comparison. All optimization parameters, except the smoothing values, were held constant at all times. These plans were then re-optimized for 100 iterations as this value is sufficient for a minimum objective function. An anisotropic analytical algorithm (AAA) was used for the final dose calculation with a grid size of 2.5 mm. For these 20 IMRT patients, 20 × 9 combinations of treatment plans were optimized, giving a total of 180 individual dose plans.

A comparative study of treatment plans was done from the treatment plan reports, dose-volume histogram (DVH) data, and the calculated radiobiological indices. The deliverability of these plans was also examined by two-dimensional (2-D) fluence comparisons between the planned and measured fluence. For a better understanding of the results, statistical tests have been carried out. We used one-way ANOVA, the column analysis method, in which the mean of each column (data for various smoothing levels) has been compared with the mean of every other column, whereby it can be concluded whether the observed variations in different figures are statistically significant. GraphPad prism (Graphpad software, San Diego, CA, USA, version 6.07) was used for the above tests, and the deviations were considered significant for p values <0.05.

2.1 Treatment plan reports and DVH

We generated treatment plan reports to obtain the total number of MUs. We performed DVH analysis to determine the near-maximum dose ($D_{2\ \%}$), the dose to 95 % of the volume ($D_{95\ \%}$) for the PTV. We also determined the maximum dose ($D_{\max}$), and the doses received by the different volumes of OARs as per the radiation therapy

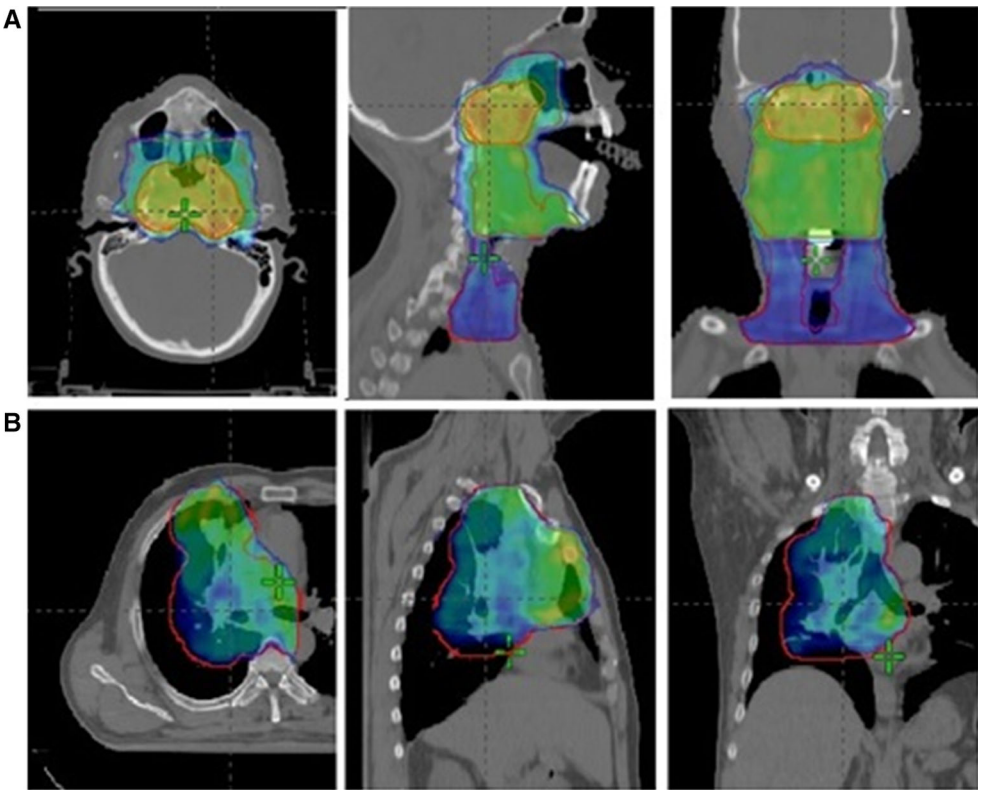

Fig. 1 Axial, coronal, and sagittal views (from *left* to *right*) of color washed isodose distributions of a **a** nasopharynx patient and **b** lung patient

Table 1 List of parameters used for calculation of EUD-based TCP and NTCP

Structure set	Volume type	End point	a	TCD_{50}/TD_{50}	γ_{50}	α/β	References
Nasopharynx-PTV	Tumor	–	−13	51.77	2.28	10	[25]
Lung-PTV	Tumor	–	−13	36.5	0.72	10	[27]
Lung	Normal	Pneumonitis	1	24.5	2	3	[23, 26]
Heart	Normal	Pericarditis	3	50	3	2	[23, 26]
Spinal cord	Normal	Myelitis	13	66.5	4	2	[25, 26]
Brainstem	Normal	Necrosis	7	65	3	3	[23, 28]
Chiasm	Normal	Blindness	25	65	3	3	[23, 28]

oncology group (RTOG) protocols. For target coverage, at least 95 % of the prescribed dose should receive more than 95 % of the PTV. The OAR constraints include volumes <1 % above 5400 cGy for the optic nerves and chiasm, a maximum dose <5400 cGy for the brainstem, and a volume of the spinal cord <1 % above 5000 cGy [17–19]. Additional constraints, including a volume of the whole lung receiving 2000 cGy (V_{2000}) < 30–35 % for lung and the volume of the heart receiving 4000 cGy (V_{4000}) < 30 % for heart were also taken care of [20, 21].

2.2 Radiobiological indices

Treatment plans can be effectively compared based on equivalent uniform dose (EUD)-based radiobiological estimates [22]. Tumor control probability (TCP) and normal tissue complication probability (NTCP) were calculated in this study. Even though there are different models for predicting the radiobiological outcome of the treatment, the EUD-based model is very simple and versatile [23]. According to Niemierko's phenomenological model, the EUD is given by [23, 24]

$$\mathrm{EUD} = \left(\sum_{i=1}\left(v_i D_i^a\right)\right)^{\frac{1}{a}}, \tag{3}$$

where a is a unitless tissue-specific parameter, whose value is negative for tumors and positive for normal structures. If $a = 1$, the EUD is the mean dose. v_i is also unitless; it represents the ith partial volume receiving dose D_i in Gy. The TCP and NTCP are calculated from the EUD as follows [23]:

$$\mathrm{TCP} = \frac{1}{1 + \left(\frac{\mathrm{TCD}_{50}}{\mathrm{EUD}}\right)^{4\gamma_{50}}}, \tag{4}$$

$$\mathrm{NTCP} = \frac{1}{1 + \left(\frac{\mathrm{TD}_{50}}{\mathrm{EUD}}\right)^{4\gamma_{50}}}. \tag{5}$$

The TCD_{50} is the tumor dose required for control of 50 % of the tumor, and TD_{50} is the tolerance dose for a 50 % complication rate at a specific time interval when the whole organ of interest (tumor or normal tissues) is homogeneously irradiated. γ_{50} is a dimensionless (%/%) parameter that describes the slope of the dose–response curve. It is also specific to both normal tissues and tumors. The parameters TCD_{50} and γ_{50} are obtained by fitting of clinical dose–response data to the EUD-based models.

The EUD-based TCP and NTCP were calculated by use of a MatLab program (The MathWorks, Inc., Natick, MA, USA) [23]. This program requires cumulative DVH data along with various radiobiological factors such as TCD_{50}, TD_{50}, a, and γ_{50}. The values of these factors used in this study are summarized in Table 1 (data were obtained from various publications [23, 25–28]).

2.3 Dose measurements

The fluence complexity has a considerable effect on the accuracy of dose delivery [14]. Therefore, we also studied the correlation of the fluence complexity with delivery accuracy. The 2-D dose distributions for each plan were calculated with a MULTICube™ phantom in Eclipse™ and compared with the corresponding measured dose distributions. The I'MRT MatriXX 2-D (IBA Dosimetry, Schwarzenbruck, Germany) array system consisting of 1020 vented parallel ion chambers, arranged in 32 × 32 grids, was used for measurements. The diameter, height, and volume of each detector were 4.5 mm, 5 mm, and 0.08 cm^3, respectively. The inherent water-equivalent build-up thickness was 3.2 mm, and the active measurement area was 24 × 24 cm^2. The spatial resolution of the detector system was 7.6 mm. This low spatial resolution due to the size of a detector and the transport of secondary electrons from the walls into the measuring volume introduces large errors in the gamma analysis of steep dose gradients. The dose points measured by the detector array were interpolated from 7.6 to 1.0 mm by use of the linear interpolation method of the IBA OmniPro IMRT verification system (IBA Dosimetry, Schwarzenbruck, Germany). The calculated 2-D fluence maps of all of the plans were transferred to the OmniPro IMRT verification system. These plans were delivered to the detector in a fixed set-up with use of the MULTICube phantom. The source-to-detector distance was 100 cm, and the thickness of the build-up and backscatter material was 10.5 and 7.5 cm, respectively.

The quantitative evaluation in terms of the gamma index (% dose difference and distance to agreement [DTA]) [29] of the measured against the TPS-calculated doses was performed for all dynamic IMRT plans. The percentage of the beam area with a gamma value smaller than one (area $\gamma < 1$ %) was obtained and tabulated. The standard passing criterion is 3 % for dose difference analysis, and the 3 mm criterion for DTA analysis (3 %/3 mm) [30]. This 3 %/3 mm passing criterion and a tighter criterion of 2 %/2 mm were evaluated in this study. The mean and standard deviation for the gamma values were calculated and compared. This will help in understanding the smoothing values which show a higher degree of deliverability.

3 Results

A detailed analysis of the treatment plans results in the following information.

3.1 Total MU

We observed that the averages of the total MUs for both study groups decreased with increasing *X*–*Y* smoothing values, as shown in Table 2. For the nasopharynx, the total number of MUs came down from 2079 ± 265.4 at $X = 0$, $Y = 0$ to 1107 ± 137.4 at $X = 100$, $Y = 100$, whereas for the lung, the corresponding decrease was from 1556 ± 490.3 to 791 ± 176.8.

3.2 DVH analysis

$D_{95\ \%}$ of the PTV obtained from the DVH had a maximum variation of only 0.6 % for the nasopharynx and 0.5 % for the lung. Similarly, the average $D_{2\ \%}$ was found to vary by 0.3 and 1.3 % for the nasopharynx and lung, respectively, when we increased smoothing from $X = 0$, $Y = 0$ to $X = 100$, $Y = 100$. Table 3 presents the average dose values (cGy) for 95 and 2 % of the PTVs of the respective

Table 2 Detailed reports of MUs generated by TPS over various fluence levels in both study groups

Smoothing levels	Nasopharynx plans			Lung plans		
	Max. MU	Min. MU	Avg. MU ± SD	Max. MU	Min. MU	Avg. MU ± SD
$X = 0$, $Y = 0$	2433	1743	2079 ± 265.4	2189	798	1556 ± 490.3
$X = 20$, $Y = 10$	2360	1693	2004 ± 244.4	2125	769	1488 ± 465.7
$X = 40$, $Y = 30$	2049	1399	1696 ± 212.4	1817	680	1240 ± 368.7
$X = 50$, $Y = 40$	1830	1253	1532 ± 180.6	1551	653	1112 ± 303.1
$X = 60$, $Y = 50$	1683	1169	1416 ± 149.1	1435	589	1011 ± 282.8
$X = 70$, $Y = 60$	1604	1089	1306 ± 150.8	1254	546	944 ± 246.9
$X = 80$, $Y = 70$	1510	1066	1239 ± 131.8	1148	536	876 ± 219.1
$X = 90$, $Y = 80$	1478	1013	1184 ± 139.2	1081	525	843 ± 203.9
$X = 100$, $Y = 100$	1415	992	1107 ± 137.4	1001	499	791 ± 176.8
p value			<0.0001			<0.0001

Max. maximum, *Min.* minimum, *Avg.* average, *SD* standard deviation

Table 3 Average doses (cGy) to 95 and 2 % of PTV obtained from DVH of both nasopharynx and lung plans

Smoothing levels	$D_{95\ \%}$ of nasopharynx plans (Avg. ± SD)	$D_{95\ \%}$ of lung plans (Avg. ± SD)	$D_{2\ \%}$ of nasopharynx plans (Avg. ± SD)	$D_{2\ \%}$ of lung plans (Avg. ± SD)
0/0	6763.3 ± 69.46	5732.0 ± 56.79	7347.6 ± 216.78	6386.7 ± 196.88
20/10	6769.1 ± 70.89	5754.7 ± 67.18	7348.5 ± 219.02	6404.2 ± 195.63
40/30	6772.4 ± 71.66	5729.6 ± 54.08	7335.1 ± 187.27	6407.2 ± 175.48
50/40	6762.6 ± 59.22	5764.5 ± 67.41	7338.7 ± 181.34	6414.4 ± 179.75
60/50	6749.4 ± 50.82	5749.6 ± 57.52	7340.6 ± 186.35	6427.1 ± 176.92
70/60	6773.3 ± 71.37	5744.4 ± 57.80	7346.1 ± 189.48	6419.2 ± 187.67
80/70	6754.2 ± 63.82	5731.6 ± 68.43	7363.8 ± 203.58	6417.4 ± 192.71
90/80	6734.4 ± 65.80	5727.4 ± 68.21	7371.0 ± 202.41	6423.8 ± 205.26
100/100	6737.8 ± 65.75	5725.7 ± 68.21	7371.4 ± 173.12	6469.1 ± 195.15
p value	0.2646	0.1158	0.1622	0.0997

No statistically significant variations were observed

groups. The maximum dose and the volume dose for various OARs were studied, and the detailed DVH data are plotted in Fig. 2.

3.3 Radiobiological indices

The average EUD and the estimated TCP varied minimally during the process of smoothing. The maximum changes observed in the average EUD and TCP of the nasopharynx plans were from 6935.8 ± 172.4 to 6868.5 ± 176.4 and from 93.4 ± 1.6 to 92.8 ± 1.7, respectively, (p values 0.1629 and 0.2103). In the case of the lung plans, the corresponding changes were from 5986.5 ± 218.7 to 5885.8 ± 272.4 in the average EUD and from 80.9 ± 1.5 to 79.4 ± 3.1 in the average TCP (p values 0.2011 and 0.2993). However, a small, but reproducible increase in the EUD and TCP values at medium smoothing levels between $X = 50$, $Y = 40$ and $X = 80$, $Y = 70$ was observed. Figure 3 depicts the variations in the average EUD and TCP with increasing smoothing levels. Radiobiological estimation of the NTCP was done for selected normal tissues, and the result is given in Table 4.

3.4 Dose map comparison

The results for the gamma passing rate for all measured smoothing levels with respect to their TPS plans for both treatment sites are summarized in Table 5. In the nasopharynx plans, the percentage of points within the passing range (γ 3 mm–3 %) is only 92.68 ± 4.52 for $X = 0$, $Y = 0$, whereas 98.55 ± 0.98 % points remain in the same range for $X = 100$, $Y = 100$ smoothing. Similarly, in the lung patients, the corresponding improvement in the percentage of points was from 93.15 ± 3.22 to 97.02 ± 1.88 for a change in smoothing from $X = 0$, $Y = 0$ to $X = 100$, $Y = 100$. Gamma passing rates using stricter gamma criteria (γ 2 mm–2 %) also exhibited substantial improvements in percentage of points from lower to higher smoothing values. In both cases, measured plans with smoothing values $X = 70$, $Y = 60$ and above showed an improved agreement with the TPS plans, as is evident in Fig. 4.

4 Discussion

In the present study, we investigated the application of the vendor-supplied fluence-smoothing interface of Eclipse™ in treatment plan optimization and related changes in the quality of nasopharynx and lung IMRT plans. The examination of 180 individually optimized plans revealed that, as smoothing was increased, the number of maximum, minimum, and average MUs decreased for both groups of patients. MUs are calculated from a term called MU factor which, in turn, is related to the complexity of the plan. A small field requires a larger number of MUs to reach the same dose as that for large fields. The large-scale modulations in complex IMRT plans require a large number of small and irregularly shaped beam segments to achieve high dose conformity. Thus, the complexity of IMRT is reflected in a large number of treatment MUs [5]. Plan complexity and smoothing are always inversely related, and any reduction in fluence complexity is highly correlated with a corresponding decrease in MUs [14]. Our results for sites with numerous critical structures and inhomogeneities agree with previous findings for various other sites [5, 7, 14, 16]. The observed decrease in the average MUs was 46.8 % for the nasopharynx and 49.2 % for the lung plans over the whole range of smoothing, which was statistically significant. However, the major contributions (37.2 and 39.3 %) are from smoothing $X = 0$, $Y = 0$ to $X = 70$, $Y = 60$. Percentages of reduction in MU from vendor-recommended smoothing to $X = 70$, $Y = 60$ plans are 23.0 and 23.9 % for the nasopharynx and lung plans, respectively. All of the above differences are statistically significant (p values <0.0001).

Another important aspect of this study is the radiobiological estimation of treatment plans. Radiobiological models were proved to be effective in predicting treatment outcome precisely by use of DVH data when compared to the uncertainty of using physical dose metrics alone for plan evaluation [22]. The results for the 90 plans investigated in each group did not show any major violations of the clinical acceptability of those plans. The estimation of TCP, which had a good correlation with the conformity index [22], also showed little or no variation with fluence smoothing. However, the observed slight improvements in both EUD and TCP from the $X = 50$, $Y = 40$ to the $X = 80$, $Y = 70$ smoothing interval was noticeable.

Although variations are observed in the D_{95} and $D_{2\ \%}$ of the PTVs (Table 3), the given method of DVH analysis may not clearly reflect the small change in the PTV volume dose. A detailed study about various OARs revealed that there was no significant difference in the organ dose values except for the D_{max} of the brainstem and spinal cord in the nasopharynx group. A statistically significant increase of D_{max} in both the brainstem and spinal cord was obtained. This is because of the increase in smoothing, which obstructs the optimizer for achieving harder constraints of the plans. The average maximum doses to the brainstem and spinal cord were increased by 5.9 and 6.7 %, respectively, for an increase in smoothing from default values to the highest levels (p values 0.0005 and 0.0255). The major changes in the D_{max} occurred approximately from $X = 70$, $Y = 60$ to the highest values in this study. The observed increase in the D_{max} of the brainstem and spinal cord from

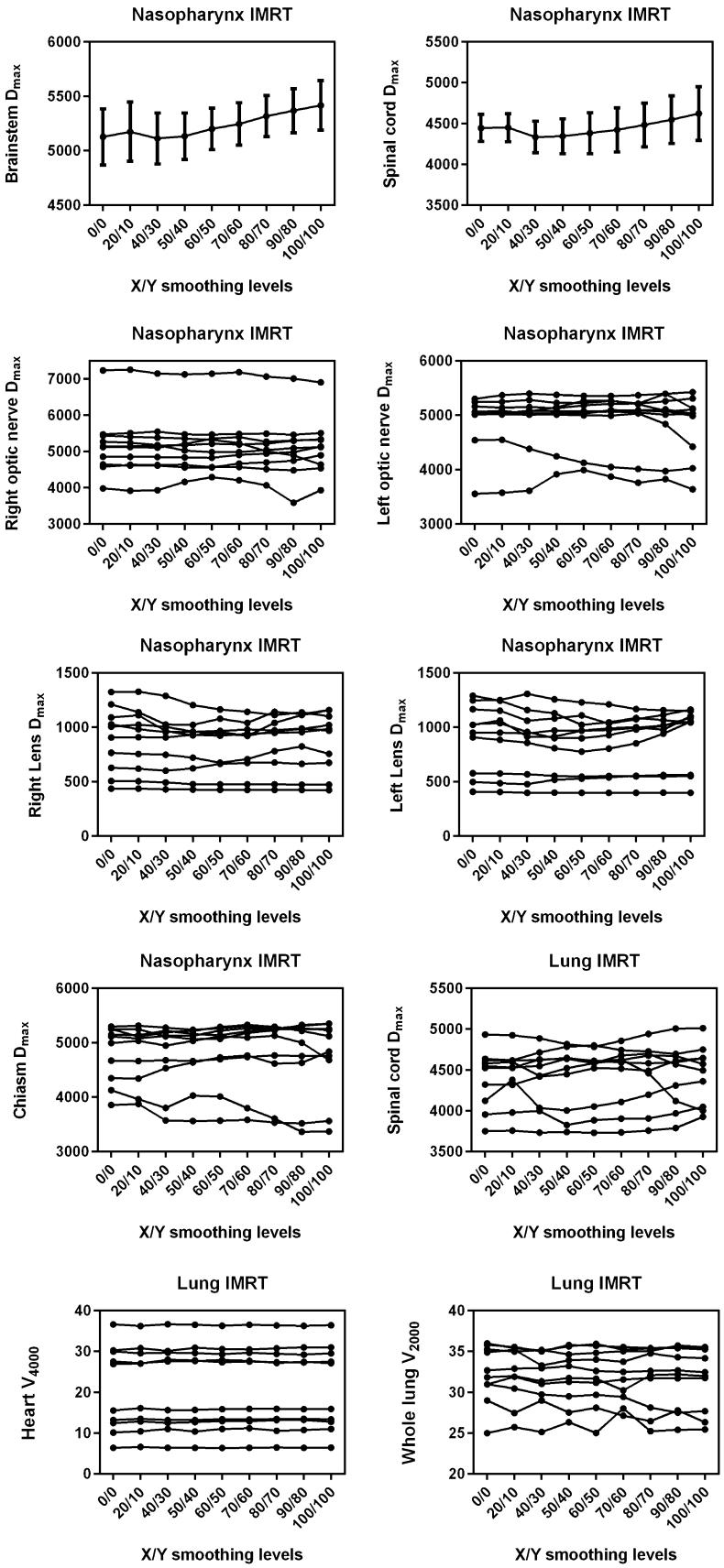

Fig. 2 Effect of smoothing on the maximum dose and the volume dose of various OARs in both study groups. D_{max} (cGy) is plotted for brainstem, spinal cord, optic nerves, chiasm, and lenses. In the case of heart and lung, respectively, the percentage of tissue volumes that received 4000 and 2000 cGy are also plotted

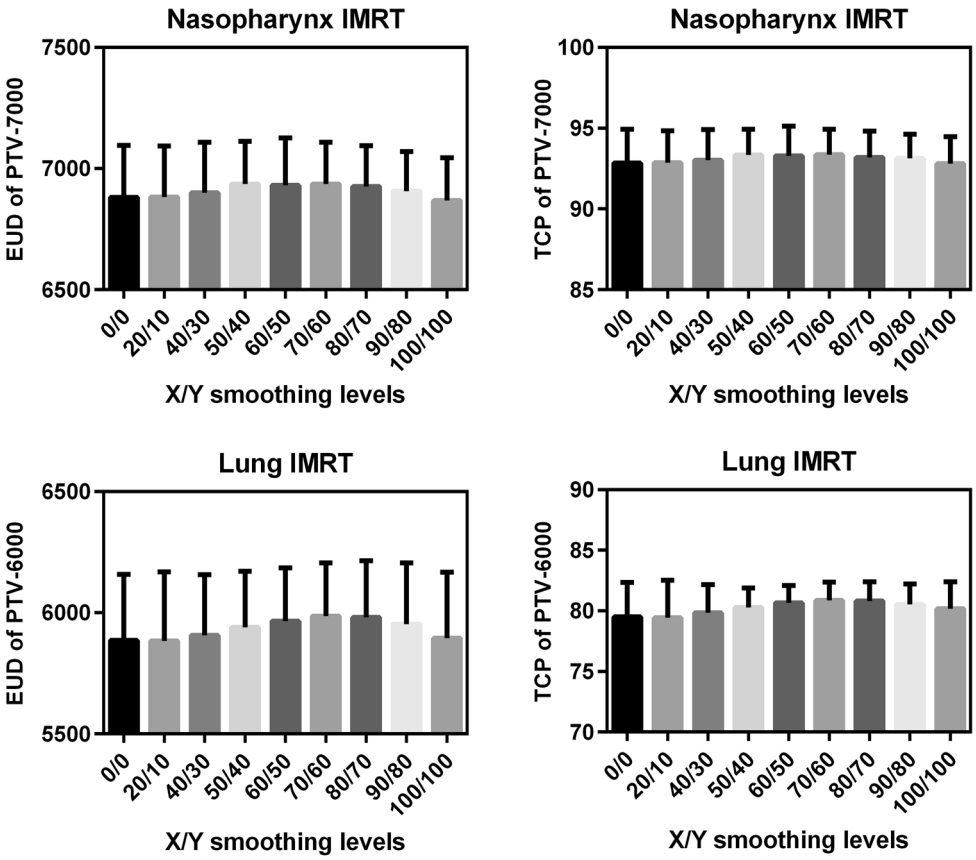

Fig. 3 Average EUD/TCP variations with increasing smoothing levels in both study groups

Table 4 Average values of EUD (cGy) and NTCP (%) for different OARs with various degrees of fluence smoothing

Smoothing levels	Brainstem		Spinal cord (nasopharynx)		Chiasm		Lung		Spinal cord (lung)		Heart	
	EUD	NTCP	EUD	NTCP	EUD	NTCP	EUD	NTCP	EUD	NTCP	EUD	NTCP
0/0	3211.0	0.0291	2750.1	0.0001	3455.1	0.1379	1583.5	6.017	2904.8	0.0005	2918.1	0.8523
20/10	3197.9	0.0286	2745.7	0.0001	3402.1	0.1214	1584.7	5.984	2896.5	0.0005	2914.5	0.8279
40/30	3169.9	0.0244	2713.6	0.0001	3388.6	0.1178	1590.8	6.287	2912.6	0.0005	2916.6	0.8426
50/40	3224.2	0.0350	2708.1	0.0001	3412.5	0.1066	1603.6	6.664	2924.5	0.0005	2931.4	0.8888
60/50	3278.3	0.0360	2762.1	0.0001	3406.0	0.1207	1620.8	7.173	2929.9	0.0006	2939.5	0.8836
70/60	3357.7	0.0467	2801.0	0.0002	3478.0	0.1549	1647.1	7.956	2927.3	0.0006	2951.0	0.8476
80/70	3362.7	0.0635	2864.1	0.0002	3455.7	0.1414	1476.5	8.592	2950.6	0.0007	2946.6	0.8298
90/80	3512.6	0.0792	2931.2	0.0003	3390.1	0.1565	1294.7	9.677	2887.9	0.0007	2921.1	0.7907
100/100	3583.3	0.0990	3005.7	0.0004	3468.0	0.1893	1701.6	10.72	2851.2	0.0007	2896.4	0.7556
p value	0.0016	0.0184	0.0417	0.0289	0.7002	0.5157	0.2928	0.2834	0.5398	0.4845	0.3964	0.6912

vendor-recommended values to $X = 70$, $Y = 60$ was 2.6 and 2.0 %, respectively (p values 0.0023 and 0.1722). The estimated EUD and NTCP of these structures showed a similar behavior. However, the analyzed dose figures for the optic nerve, optic chiasm, and lenses in the nasopharynx patients and those of the spinal cord, lung, and heart in the lung patients did not show any trend or reproducibility over the entire smoothing range.

The measurements and evaluation processes with the MatriXX 2-D system can be used for quantifying the degree of deliverability of the TPS-generated plans. The results of a 2-D dose comparison show gradual improvements in the percentage of points satisfying the passing criterion with respect to the increased fluence smoothing. This is clearly shown in Fig. 5 for a particular patient in each of the groups (four levels of successive smoothing are given). Low smoothing parameters in Eclipse™ make the fluences appear more complex, and the gamma passing rate decreases with increasing complexity of the plan. Another interesting observation is the similarity of the gamma

Table 5 Gamma results—summary of comparison between TPS fluence and that measured with MatriXX 2-D array system

Smoothing levels	% of pixels passed (γ <1) in nasopharynx plans		% of pixels passed (γ <1) in lung plans	
	3 %–3 mm	2 %–2 mm	3 %–3 mm	2 %–2 mm
00/00	92.68 ± 4.52	70.41 ± 8.48	93.15 ± 3.22	65.51 ± 7.72
20/10	94.67 ± 3.04	73.70 ± 7.58	94.05 ± 2.66	67.34 ± 7.62
40/30	95.78 ± 2.25	77.06 ± 6.84	94.93 ± 2.45	69.39 ± 7.89
50/40	96.15 ± 1.83	77.32 ± 6.84	95.08 ± 2.14	71.02 ± 6.89
60/50	96.85 ± 1.48	78.63 ± 5.59	95.68 ± 1.86	71.03 ± 8.88
70/60	98.13 ± 0.97	81.77 ± 5.56	96.80 ± 1.56	74.54 ± 6.90
80/70	98.12 ± 0.87	81.89 ± 4.73	96.66 ± 1.66	74.50 ± 7.56
90/80	98.25 ± 0.93	82.46 ± 5.28	96.68 ± 1.85	74.77 ± 7.51
100/100	98.55 ± 0.98	85.47 ± 5.35	97.02 ± 1.88	75.66 ± 7.49
p value	0.0027	<0.0001	<0.0001	0.0005

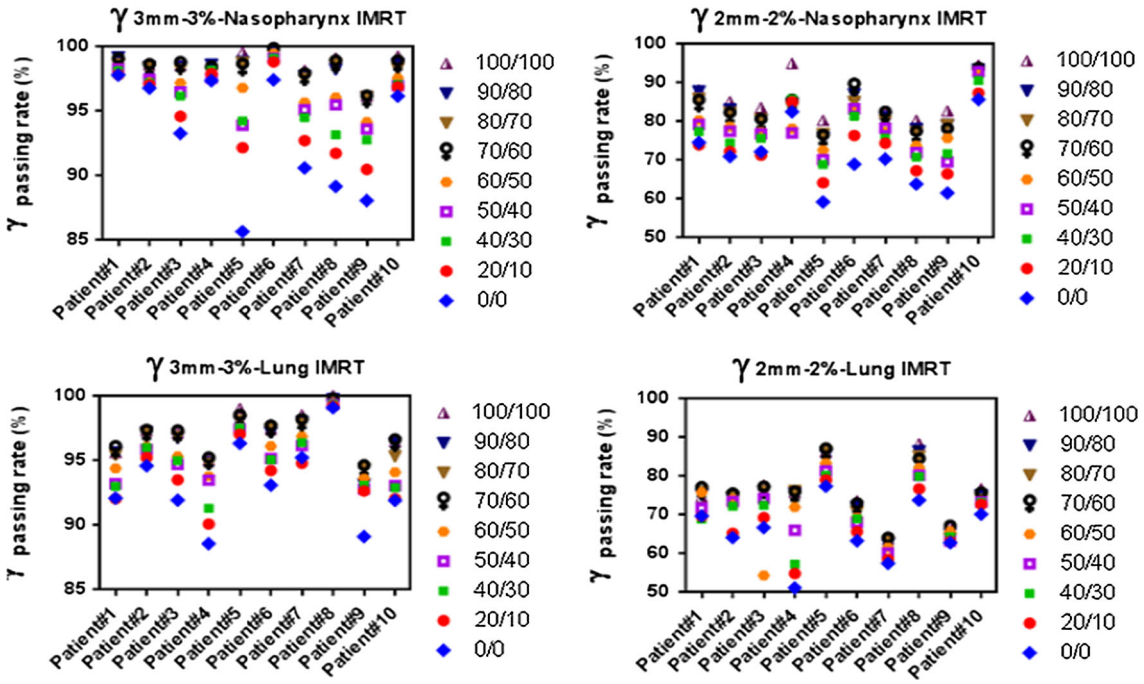

Fig. 4 Dosimetric comparison of different smoothing plans with their measured distributions. Smoothing improved the agreement between measured and TPS plans in both groups

results for the fluence levels of $X = 70$, $Y = 60$ or above (except for $X = 100$, $Y = 100$) in any combinations, which can be well understood from Table 5.

In a number of studies, the use of fluence-smoothing function of commercial IMRT planning systems has been investigated. A study performed by Armoogum [16] examined the effect of fluence smoothing with an inverse-planning IMRT software (Helios, Eclipse version 8.9.09, Varian Medical Systems) for a cohort of prostate and of head and neck patients. The average leaf-pair opening (LPO), MU factor, and total number of MUs were studied with different fluence-smoothing values. The study showed that an increase in smoothing results in a significant reduction in MUs and a definite increase in average LPO due to the reduced plan complexity. Another study by Anker et al. [12] compared the behavior of these smoothing functions in three inverse TPSs (Eclipse-Varian Medical Systems, Palo Alto, CA, USA; BrainScan, BrainLAB AG, Feldkirchen, Germany; and CORVUS, Best Nomos, Pittsburg, PA, USA) for four different IMRT plans. This

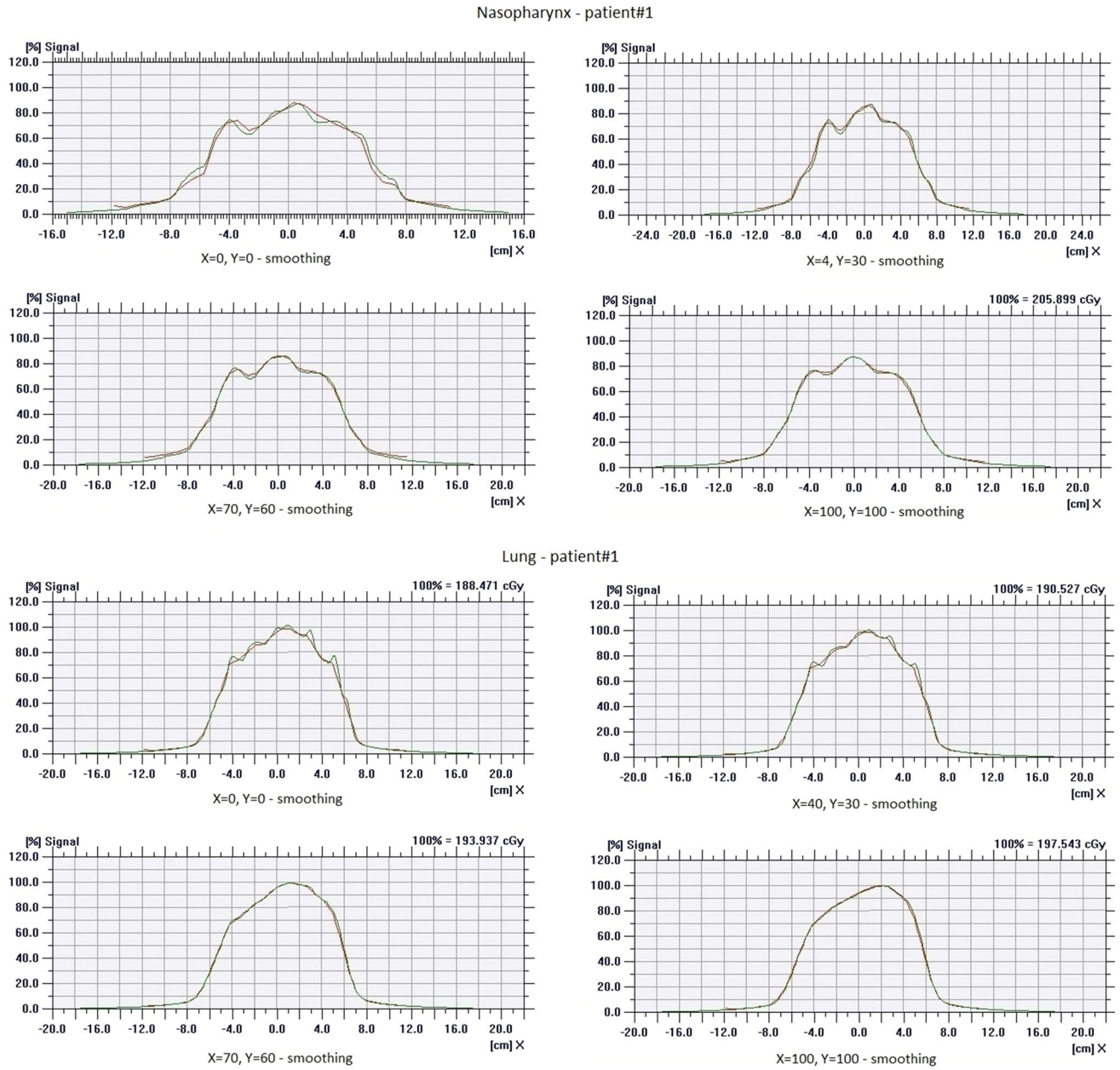

Fig. 5 Comparison between TPS fluence and that measured with the MatriXX 2-D array system for a nasopharynx and lung IMRT plan with 4 different levels of smoothing. A better correlation is observed toward maximum smoothing

analysis was essentially done for understanding of each TPS's smoothing algorithm by discussing them in parallel. Within the wide range of fluence smoothing from $X, Y = 0$ to $X, Y = 999$, they found a significant degradation in plan conformality at $X \geq 150$, $Y \geq 150$ smoothing levels. All OARs showed a higher $D_{\max}$ at $X = 200$, $Y = 200$ and they have recommended for considering the increasing of smoothing levels, by keeping $X \leq 80$ and $Y \leq 60$, to achieve the benefit of decreasing complexity without compromising PTV coverage or OAR sparing. The behavior of smoothing functions in our study is in good agreement with their findings. We have done our studies on two particular sites, and these were chosen because of their relatively highly complex and heterogeneous dose distribution. In contrast to those purely computational studies, this publication verifies the deliverability of treatment plans by actual measurement based on a larger set of data (180 plans). Our study not only is limited to physical dose evaluation, but also investigates the impact of fluence complexity on radiobiology based plan quality parameters.

The effect of smoothing on more popular prostate groups was done by the above authors. The behavior of the prostate plans was consistent with that of other sites. A more noticeable decrease in the MUs was observed with an increase in smoothing [16]. However, the quality degradation of these plans started for smoothing values above $X = 60$, $Y = 45$ [12].

A recommendation for good IMRT practice is always to minimize the treatment MUs as far as possible. For every patient, there may be an optimum complexity level needed for achieving an acceptable plan. Obviously, this complexity will be decided by the required dose distribution leading to tumor lethality and the chosen constraints for the OAR. However, any additional complexity resulting in noise in the fluence map causes a significant increase in MUs, with little or no plan refinement. It is essential to determine the optimum values of smoothing for routine planning without sacrificing the quality of the treatment plans, especially for complex and irregular anatomic regions.

Even though it may not be possible to suggest the exact smoothing values for Eclipse^{TM}, our studies can give recommendations for changing the standard smoothing values to some higher values. Interestingly, all smoothing combinations of the current study, starting from $X = 40$, $Y = 30$, produced a clinically acceptable plan in terms of both tumor control and normal-tissue complications. However, an optimum smoothing value of $X = 70$, $Y = 60$ can be recommended based on the observations of outstanding differences in MUs, along with the slight improvements in the EUD and a lesser deviation of the D_{max} of certain critical structures from the default plans. The noted differences of about 23.0 and 23.9 % in the respective treatment MUs are exceptionally high. The transformation of smoothing values from default to $X = 70$, $Y = 60$ saved around 390 MU (nasopharynx) and 290 MU (lung) per fraction. This will result in a reduction of approximately 32 and 21 min, respectively, in the total radiation-beam-on time for the entire course of a patient treatment. Thus, this smoothing level can replace the default level without significant deviations in the plan quality, but with a considerable decrease in MU values and in total "beam-on" time.

The Eclipse^{TM} TPS uses both a dose-volume optimizer (DVO) algorithm for evaluation of dose for optimization and a more accurate AAA for final volume dose calculation. The fast optimization DVO algorithm introduces an optimization convergence error [31] when the dose calculation is in the build-up region or is due to the calculation of lateral scatter. Therefore, the final AAA-based dose calculation DVH may differ from the optimized DVO-based DVH for the IMRT plans with a PTV in the head and neck or lung region. This error can be minimized by performing a large number of iterations within the DVO, followed by a periodic correction [32] to the final dose calculation. The standard practice of optimization in our institution is the use of a relatively larger number of iterations for nasopharynx and lung plans where the PTVs are not in the vicinity of electronic equilibrium. It is understood that a large number of iterations often results in increasing MUs and a smaller MLC gap width. We also studied the impact of smoothing on MUs for a small number of iterations (50), and we found a slight and less marked, but statistically significant, decrease in MUs with increasing smoothing. However, this study was done by use of 100 iterations matching with our clinical cases that yields a minimum cost function for the nasopharynx and lung plans. Also, this study was restricted to a particular plan setting which influences the total objective function. The iterative method for reaching a minimum cost function is influenced by many variables, such as the optimization priority, user-defined dose volume constraints, and smoothing. The relative contribution of smoothing penalty and the structure-dose penalty were varied and found to have little effect on plan quality [12]. Further work is required for finding the effect of smoothing in the user-defined dose-volume constraints for different disease sites.

5 Conclusions

The study of nasopharynx and lung IMRT treatment plans with different scenarios of fluence levels helped us to understand the effect of user-interfaced fluence smoothing with the Eclipse^{TM} TPS in detail. This scientific endeavor clearly showed a significant reduction in treatment MUs without any considerable variations in OAR sparing. The estimated biological outcome and DVH analysis do not recommend the rejection of any combinations of smoothing from vendor-recommended levels to the maximum values of this study. However, the observed efficiency of plan deliverability in terms of the gamma index toward higher smoothing levels promotes the idea of advancing the smoothing levels from $X = 40$, $Y = 30$ to $X = 70$, $Y = 60$. In addition, an appreciable reduction in MUs without critical deviations in the plan quality powerfully supports the recommendation of using smoothing levels up to $X = 70$ and $Y = 60$, at least for the anatomic regions studied.

Compliance with ethical standards

Conflict of interest The authors declare that they have no conflict of interest.

References

1. Delaney G, Jacob S, Featherstone C, Barton M. The role of radiotherapy in cancer treatment. Cancer. 2005;104:1129–37. doi:10.1002/cncr.21324.
2. Varian Medical Systems. External beam planning reference guide eclipse. Palo Alto, CA: Varian medical systems; 2007.
3. Dobler B, et al. Direct machine parameter optimization for intensity modulated radiation therapy (IMRT) of oropharyngeal cancer—a planning study. J Appl Clin Med Phys. 2009;10(4):3066.
4. Broderick M, Leech M, Coffey M. Direct aperture optimization as a means of reducing the complexity of Intensity Modulated Radiation Therapy plans. Radiat Oncol. 2009;4(8):1–7.
5. Mohan R, Arnfield M, Tong S, Wu Q, Siebers J. The impact of fluctuations in intensity patterns on the number of monitor units and the quality and accuracy of intensity modulated radiotherapy. Med Phys. 2000;27:1226–37.
6. Hall EJ, Wu C. Radiation induced second cancers: the impact of 3DCRT and IMRT. Int J Radiat Oncol Biol Phys. 2003;56:83–8.
7. Spirou SV, Fournier-Bidoz N, Yang J, Chui CS, Ling CC. Smoothing intensity modulated beam profiles to improve the efficiency of delivery. Med Phys. 2001;28:2105–12.
8. Sun X, Xia P. A new smoothing procedure to reduce delivery segments for static MLC-based IMRT planning. Med Phys. 2004;31:1158–65.
9. Webb S, Convery DJ, Evans PM. Inverse planning with constraints to generate smoothed intensity modulated beams. Phys Med Biol. 1998;43(10):2785–94.
10. Matuszak MM, Larsen EW, Fraass BA. Reduction of IMRT beam complexity through the use of beam modulation penalties in the objective function. Med Phys. 2007;34(2):507–20.
11. Matuszak MM, Larsen EW, Jee K, McShan DL, Fraass BA. Adaptive diffusion smoothing: a diffusion-based method to reduce IMRT field complexity. Med Phys. 2008;35(4):1532–46.
12. Anker CJ, Wang B, Tobler M, Chapek J, et al. Evaluation of fluence smoothing feature for three IMRT planning systems. J Appl Clin Med Phys. 2010;11:3035.
13. Varian Medical Systems. Reference guide for eclipse algorithms: Vision eclipse—external beam planning v6.5. Palo Alto, CA: Varian Medical Systems; 2004.
14. Nicolini G, Fogliata A, Vanetti E, et al. What is an acceptably smoothed fluence? Dosimetric and delivery considerations for dynamic sliding window IMRT. Radiat Oncol. 2007. doi:10.1186/1748-717X-242.
15. Mayo C, Urie M. Eclipse IMRT: a practical treatment planning guide. Las vegas: Varian Medical Systems; 2004. p. 24–7.
16. Armoogum KS. Effect of smoothing on treatment plan efficiency in IMRT: eclipse Helios^{TM} dose optimisation. J Radiother Pract. 2012;11(04):229–38.
17. Mayo C, Yorke E, Merchant TE. Radiation associated brainstem injury. Int J Radiat Oncol Biol Phys. 2010;76:S36–41.
18. Mayo C, Martel MK, Marks LB, Flickinger J, Nam J, Kirkpatrick J. Radiation dose-volume effects of optic nerves and chiasm. Int J Radiat Oncol Biol Phys. 2010;76:S28–35.
19. Kirkpatrick JP, van der Kogel AJ, Schultheiss TE. Radiation dose–volume effects in the spinal cord. Int J Radiat Oncol Biol Phys. 2010;76:S42–9.
20. Marks LB, Bentzen SM, Deasy JO, et al. Radiation dose-volume effects in the lung. Int J Radiat Oncol Biol Phys. 2010;76:70–6.
21. Matzinger O, Gerber E, Bernstein Z, et al. EORTC-ROG expert opinion. Radiotherapy volume and treatment guidelines for neo-adjuvant radiation of adenocarcinomas of the gastroesophageal junction and the stomach. Radiother Oncol. 2009;92:164–75.
22. Anbumani S, Raj NA, Prabhakar GS, et al. Quantification of uncertainties in conventional plan evaluation methods in Intensity Modulated Radiation Therapy. J BUON. 2014;19(1):297–303.
23. Gay HA, Niemierko A. A free program for calculating EUD-based NTCP and TCP in external beam radiotherapy. Phys Med. 2007;23(3–4):115–25.
24. Niemierko Andrzej. A generalized concept of equivalent uniform dose (EUD). Med Phys. 1999;26(6):1100.
25. Oinam AS, et al. Dose volume histogram analysis and comparison of different radiobiological models using in-house developed software. J Med Phys. 2011;36(4):220.
26. Rana S, Rogers K. Radiobiological evaluation of dose calculation algorithms in Rapid Arc planning of esophageal cancer treatment plans. Journal of Solid Tumors. 2013;3(3):44.
27. Fleckenstein J, et al. Dose distribution and tumor control probability in out-of-field lymph node stations in intensity modulated radiotherapy (IMRT) vs 3D-conformal radiotherapy (3D-CRT) of non-small-cell lung cancer: an in silico analysis. Radiation Oncology. 2015;10(1):178.
28. Kehwar TS. Analytical approach to estimate normal tissue complication probability using best fit of normal tissue tolerance doses into the NTCP equation of the linear quadratic model. J Cancer Res Ther. 2005;1(3):168.
29. Low DA, Harms WB, Mutic S, Purdy JA. A technique for the quantitative evaluation of dose distributions. Med Phys. 1998;25(5):656–61.
30. Nelms BE, Simon JA. A survey on IMRT QA analysis. J App Clin Med Phys. 2007;8(3):76–90.
31. Robert J, Keall PJ, Siebers Jeffrey V. The effect of dose calculation accuracy on inverse treatment planning. Phys Med Biol. 2002;47(3):391.
32. Zacarias AS, Mills MD. Algorithm for correcting optimization convergence errors in Eclipse. J Appl Clin Med Phys. 2009;10(4):3061.